

## Quantum-Dot/Aptamer-Based Ultrasensitive Multi-Analyte Electrochemical Biosensor

Jacob A. Hansen,<sup>†‡</sup> Joseph Wang,<sup>\*†</sup> Abdel-Nasser Kawde,<sup>†</sup> Yun Xiang,<sup>†</sup> Kurt V. Gothelf,<sup>‡</sup> and Greg Collins<sup>§</sup>

*Departments of Chemical and Material Engineering and of Chemistry and Biochemistry, Biodesign Institute, Arizona State University, Tempe, Arizona 85287-5801, Interdisciplinary Nanoscience Center (iNANO), Department of Chemistry, Langelandsgade 140, Aarhus University, 8000 Aarhus C, Denmark, and Naval Research Laboratory, Chemistry Division, Washington, D.C. 20375*

Received January 1, 2006; E-mail: joseph.wang@asu.edu

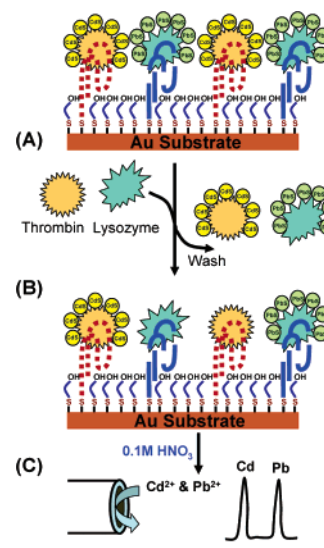
Aptamers hold great promise for the biosensing of disease-related proteins and for developing protein arrays.<sup>1,2</sup> These artificial nucleic acid ligands appear as attractive alternatives to antibodies owing to their relative ease of isolation and modification, tailored binding affinity, and resistance against denaturation. Optical or electrochemical aptamer biosensors based on enzyme,<sup>3,4</sup> fluorophore,<sup>5</sup> or nanoparticle<sup>6,7</sup> labels or on a binding-induced label-free detection<sup>8–10</sup> have been developed in recent years. These aptamer biosensors are single-analyte devices and offer detection limits down to the nanomolar level. Multi-analyte aptamer-based devices, with lower detection limits, are highly desired for measuring a large panel of disease markers present at ultralow levels during early stages of the disease progress.

Herein, we present how one can use nanocrystal tracers for designing multi-analyte electrochemical aptamer biosensors with subpicomolar (attomole) detection limits. Owing to their unique properties, quantum-dot (QD) semiconductor nanocrystals have generated considerable interest for optical DNA detection.<sup>11</sup> Recent activity has demonstrated the utility of such inorganic nanoparticles for enhanced electrochemical detection of DNA hybridization,<sup>12</sup> for electrical coding of single nucleotide polymorphisms (SNP),<sup>13</sup> and for electrochemical sandwich immunoassays of proteins.<sup>14</sup> Such nanocrystals offer an electrodiverse population of electrical tags as needed for multiplexed bioanalysis. Four encoding nanoparticles (cadmium sulfide, zinc sulfide, copper sulfide, and lead sulfide) were thus used to differentiate the signals of four DNA targets, SNPs, or antigens in connection to stripping voltammetric measurements of the corresponding metals.

The new multiple protein aptamer-based biosensing capability is coupled to the enormous amplification feature of nanoparticle-based electrochemical stripping measurements<sup>15</sup> to yield remarkably low (attomole) detection limits. This is accomplished using a simple single-step displacement assay (Scheme 1), involving the co-immobilization of several thiolated aptamers, along with binding of the corresponding QD-tagged proteins on a gold surface (A), addition of the protein sample (B), and monitoring the displacement through electrochemical detection of the remaining nanocrystals (C). Such electronic transduction of aptamer–protein interactions is extremely attractive for meeting the low power, size, and cost requirements of decentralized diagnostic systems. Unlike two-step sandwich assays used in early QD-based electronic hybridization<sup>12</sup> or immunoassays<sup>14</sup>, the new aptamer biosensor protocol relies on a single-step displacement protocol.

Single-analyte sensing was used first to assess the sensitivity and selectivity of the new device. The remarkable sensitivity accrued

**Scheme 1.** Operation of the Aptamer/Quantum-Dot-Based Dual-Analyte Displacement Assay, Involving Displacement of the Tagged Proteins by the Target Analytes<sup>a</sup>



<sup>a</sup> (A) Mixed monolayer of thiolated aptamers on the gold substrate with the bound protein–QD conjugates; (B) sample addition and displacement of the tagged proteins; (C) dissolution of the remaining captured nanocrystals followed by their electrochemical-stripping detection at a coated glassy carbon electrode. See Supporting Information for full details.

from the electrochemical stripping detection of the nanocrystal tracers is indicated from Figure 1A that displays typical voltammograms for 0 (a), 100 (b), and 500 (c) ng L<sup>-1</sup> of the thrombin target. Distinctly smaller cadmium peaks, corresponding to the remaining fractions of the undisplaced nanocrystals, are observed in the presence of low concentrations of the target protein (b, c). The resulting calibration plot (shown in Figure 1B) is characteristic of displacement assays, with a fast decrease of the peak current up to 200 ng L<sup>-1</sup> and a slower one thereafter. Analytically useful concentration dependence, extending from 20 to 500 ng L<sup>-1</sup>, is observed, along with a detection limit of 20 ng L<sup>-1</sup> (0.5 pM). Such detection limit corresponds to 54.5 attomole (2 pg) in the 100 μL sample. Accordingly, the new protocol allows assays of samples with target concentrations that are 3–4 orders of magnitude lower than those (1–6.4 nM) obtained with the most advanced aptamer biosensors reported to date.<sup>3–10</sup> A lower sensitivity was observed in an analogous competition assay (not shown). Unlike antibody-based displacement immunoassays that are inherently not sensitive,<sup>16</sup> aptamers offer great promise for sensitive displacement assays since the tagged protein has a significantly lower affinity to the aptamer compared to the unmodified analyte.<sup>4</sup>

<sup>†</sup> Arizona State University.

<sup>‡</sup> Aarhus University.

<sup>§</sup> Naval Research Laboratory.

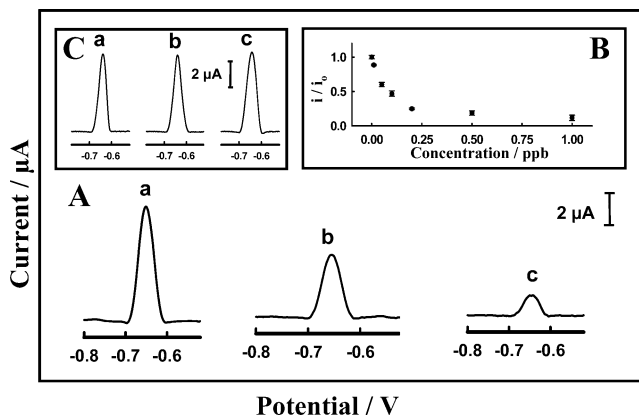


**Figure 1.** (A) Square-wave stripping voltammograms for different concentrations of thrombin: 0 (a), 100 (b), and 500 (c)  $\text{ng L}^{-1}$ . (B) The resulting calibration plot. (C) Assessment of the selectivity using nontarget proteins: (a) control (no analyte or interference), (b)  $25 \mu\text{g L}^{-1}$  BSA, and (c)  $25 \mu\text{g L}^{-1}$  IgG. Dissolution of the QDs (conjugated to the undisplaced protein molecules) was carried out by the addition of  $\text{HNO}_3$  ( $100 \mu\text{L}$ ,  $0.1 \text{ M}$ ) and sonication for 1 h. The resulting solution was transferred to a 1 mL electrochemical cell containing  $900 \mu\text{L}$  of acetate buffer ( $0.1 \text{ M}$ ,  $\text{pH } 4.6$ ) and  $10 \text{ ppm}$  mercury(II). Electrochemical stripping detection proceeded after 1 min pretreatment at  $+0.6 \text{ V}$ , 2 min accumulation at  $-1.2 \text{ V}$ , and scanning the potential to  $-0.25 \text{ V}$ .

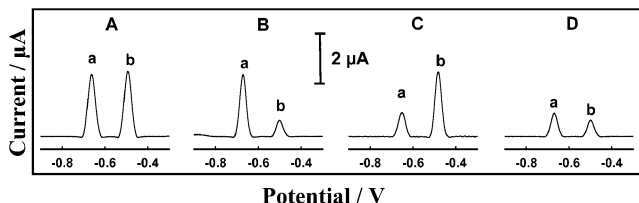


**Figure 2.** Simultaneous bioelectronic detection of lysozyme and thrombin. Square-wave stripping voltammograms obtained after additions of (A)  $0 \mu\text{g L}^{-1}$  protein, (B)  $1 \mu\text{g L}^{-1}$  lysozyme, (C)  $0.5 \mu\text{g L}^{-1}$  thrombin, and (D) a mixture of  $1 \mu\text{g L}^{-1}$  lysozyme (a) and  $0.5 \mu\text{g L}^{-1}$  thrombin (b). Conditions as in Figure 1.

The remarkably high sensitivity reflects also the presence of numerous nanocrystals per tagged protein molecule and the “built-in” preconcentration of the electrochemical stripping transduction mode. The extremely low detection limits are coupled with high selectivity. Figure 1C shows voltammograms for a blank solution (a), as well as for  $25 \mu\text{g L}^{-1}$  nontarget BSA (b) and IgG (c). Despite their relatively high concentration, these proteins have no effect upon the response (b and c vs a). Note, for comparison, the well defined response observed in Figure 1A,b for a significantly (250-fold) lower concentration of the thrombin target. Such attractive behavior reflects the absence of nonspecific adsorption effects and is attributed to the highly dense mixed monolayer on the gold surface, including the blocking action of its hydrophilic 6-mercapto-1-hexanol component.<sup>17</sup> A series of six parallel measurements of  $100 \text{ ng L}^{-1}$  thrombin yielded a relative standard deviation of 5%, reflecting the reproducibility of the protocol.

Figure 2 demonstrates the ability of the biosensor to detect simultaneously trace levels of multiple proteins. This is illustrated for the dual-analyte detection of thrombin (a) or lysozyme (b) in connection to CdS and PbS nanocrystal tracers, respectively, along with co-immobilization of the corresponding aptamers (Scheme 1).

The position and size of the corresponding metal peaks reflect the identity and concentration of the corresponding protein target. For example, additions of trace levels of lysozyme or thrombin resulted in substantial (75 and 60%) diminutions of the corresponding lead and cadmium peaks (B and C, respectively, vs A). No apparent change in the response of the second tag is observed, indicating negligible cross interferences. In contrast, the simultaneous addition of both proteins resulted in similar reductions of both metal peaks (D). The cadmium and lead peaks are sharp and well resolved. Up to five to six protein targets are thus expected to be measured simultaneously in a single run, based on the number of nonoverlapping metal peaks that can be accommodated within a potential window of ca.  $1.10 \text{ V}$ . The concept can be further scaled up by using a parallel high-throughput operation, with multiple microwells carrying out simultaneous measurements.

In conclusion, the coupling of aptamers with the coding and amplification features of inorganic nanocrystals was shown for the first time to offer a highly sensitive and selective simultaneous bioelectronic detection of several protein targets. While the concept has been demonstrated for dual-analyte sensing, it could be readily expanded for the simultaneous measurement of a large panel of proteins. The high sensitivity of such a nanoparticle-based electrochemical sensing protocol opens up the possibility of using aptamers for detecting ultratrace levels of biomarkers that cannot be measured by conventional methods and could lead to an early detection of the disease. Given that aptamer-based electrochemical sensors represent a relatively unexplored field, we expect many exciting opportunities in future aptamer-based electrochemical biosensors.

**Acknowledgment.** This research was supported by grants from the National Science Foundation (Grant No. CHE 0506529), and from the National Institutes of Health (Award Numbers R01A 1056047-02 and R01 EP 0002189).

**Supporting Information Available:** Related instrumentation, reagents, immobilization schemes and procedures. This material is available free of charge via the Internet at <http://pubs.acs.org>.

## References

- (1) Mukhopadhyay, R. *Anal. Chem.* **2005**, *77*, 115A.
- (2) Jayasena, S. D. *Clin. Chem.* **1999**, *45*, 1650.
- (3) Ikebukuro, K.; Kiyohara, C.; Sode, K. *Biosens. Bioelectron.* **2005**, *20*, 2168.
- (4) Baldrich, E.; Acero, J. L.; Reekmans, G.; Laureyn, W.; O'Sullivan, C. K. *Anal. Chem.* **2004**, *76*, 7053.
- (5) Nutio, R.; Li, Y. *J. Am. Chem. Soc.* **2003**, *125*, 4771.
- (6) Pavlov, V.; Xiao, Y.; Shlyabovskiy, B.; Willner, I. *J. Am. Chem. Soc.* **2004**, *126*, 11768.
- (7) Levy, M.; Cater, S. F.; Ellington, A. D. *ChemBioChem* **2005**, *6*, 2163.
- (8) Xiao, Y.; Lubin, A. A.; Heeger, A. J.; Plaxco, K. W. *Angew. Chem., Int. Ed.* **2005**, *117*, 5592.
- (9) Xu, D. K.; Xu, D. W.; Yu, X. B.; Liu, Z.; He, W.; Ma, Z. *Anal. Chem.* **2004**, *76*, 5107.
- (10) Rodriguez, M. C.; Kawde, A.; Wang, J. *Chem. Commun.* **2005**, *34*, 4267.
- (11) Han, M.; Gao, X.; Su, J.; Nie, S. *Nat. Biotechnol.* **2001**, *19*, 631.
- (12) Wang, J.; Liu, G.; Merkoçi, A. *J. Am. Chem. Soc.* **2003**, *125*, 3214.
- (13) Wang, J.; Lee, T.; Liu, G. *J. Am. Chem. Soc.* **2005**, *127*, 38.
- (14) Liu, G.; Wang, J.; Kim, J.; Jan, M.; Collins, G. *Anal. Chem.* **2004**, *76*, 7126.
- (15) Wang, J. *Small* **2005**, *1*, 1036.
- (16) Gerdes, M.; Mausel, M.; Spener, F. *Anal. Biochem.* **1997**, *252*, 198.
- (17) Levicky, R.; Herne, T.; Tarlov, M.; Satija, S. *J. Am. Chem. Soc.* **1998**, *120*, 9787.

JA060005H